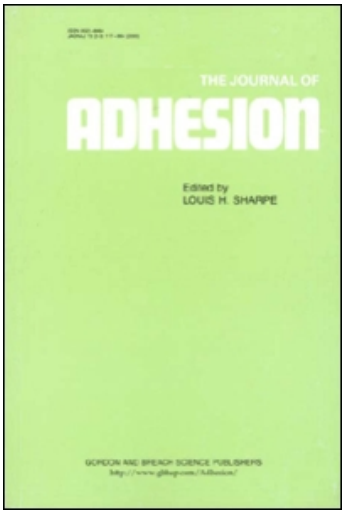

The Journal of Adhesion
Publication details, including instructions for authors and subscription information:
http://www.informaworld.com/smpp/title~content=t713453635

Chemistry of the Interface Between Aluminum and Polyester Films

James D. Rancourt[a]; James B. Hollenhead[a]; Larry T. Taylor[a]
[a] Department of Chemistry, Virginia Polytechnic Institute and State University, Blacksburg, Virginia, U.S.A.

To cite this Article Rancourt, James D. , Hollenhead, James B. and Taylor, Larry T.(1993) 'Chemistry of the Interface Between Aluminum and Polyester Films', The Journal of Adhesion, 40: 2, 267 — 285
To link to this Article: DOI: 10.1080/00218469308031289
URL: http://dx.doi.org/10.1080/00218469308031289

J. Adhesion, 1993, Vol. 40, pp. 267–285
Reprints available directly from the publisher
Photocopying permitted by license only

Printed in the United States of America.

Chemistry of the Interface Between Aluminum and Polyester Films*

JAMES D. RANCOURT, JAMES B. HOLLENHEAD and LARRY T. TAYLOR**

Department of Chemistry, Virginia Polytechnic Institute and State University, Blacksburg, Virginia 24061, U.S.A.

(Received June 5, 1992; in final form November 18, 1992)

It has been observed that the adhesion between vacuum-evaporated aluminum and poly(ethylene isophthalate-co-ethylene sodium sulfoisophthalate) copolymer is approximately five times greater than the adhesion between vacuum-evaporated aluminum and biaxially-oriented poly(ethylene terephthalate) film. To describe the interface between the aluminum and these polymeric substrates, thermoanalytical, spectroscopic and microscopic techniques have been applied. Definite changes in surface elemental composition and chemical functionality occur upon metallization of the polymer films. Aluminized samples contained two new oxygen functionalities; one due to the aluminum oxide and the other due to an organoaluminum species. Thermal degradation, as may occur during vacuum evaporation, would be expected to yield a carboxylic acid endgroup and a vinyl endgroup for each chain scission reaction that occurred. Reaction of aluminum with these carboxylic acid endgroups is thought to be responsible for the organoaluminum oxygen peak that was observed. Based on the XPS data, however, the level of this new functionality was comparable for both types of polyester film. Thus, this new functionality may be involved in promoting aluminum/polyester adhesion, but by itself cannot explain the differences in the level of adhesion that are attained. It appears, based on the transmission electron micrographs, that the aluminum deposit penetrates the copolymer coating to a greater depth than it does the PET. The greater level of penetration could be responsible for the greater adhesion obtained between vacuum-evaporated aluminum and the copolymer film compared with the level of adhesion obtained with the PET film. Based on this work, it appears that the adhesion of the vacuum-evaporated aluminum to both polyesters has a similar chemical component (type and amount) but a different extent of the mechanical component.

KEY WORDS vacuum evaporation; aluminized polyester; surface analysis; aluminum carboxylate formation; interface characterization; aluminum deposition.

INTRODUCTION

The performance of metallized polymeric films may suffer due to poor metal-to-polymer adhesion. Numerous procedures that enhance the level of adhesion attained between plastics and metals have been developed. These treatments include for example: flame treatment,[1] electrostatic discharge,[2] electrostatic discharge in the presence of monomers,[3] chemical etching,[4] UV irradiation,[5] metal or polymer

*Presented at the Fifteenth Annual Meeting of The Adhesion Society, Inc., Hilton Head Island, South Carolina, U.S.A., February 17–19, 1992.

**Corresponding author.

coating[6-9] and plasma treatment.[10] Polymer coatings that have been utilized to enhance adhesion contain for example, amine,[7] carboxylic acid,[8] or sulfonyl groups.[9]

Although many specific metal/polymer systems have been studied by researchers, the influence of the polymeric substrate on the structure of the deposited metal and the factors controlling metal/polymer adhesion remain incompletely understood.[11] Toward understanding the physical structure and interfacial chemistry that may occur in metallized systems numerous approaches have been taken by workers. Ideally, one wants to be able to probe directly the interface region of industrially-prepared samples. However, the analytical techniques that can probe samples of this type are limited. Thus, typically, custom-prepared systems are necessary to simulate industrially-prepared materials.

Good adhesion between chromium, nickel, titanium and aluminum with polyimide has been observed and attributed to the formation of metal-oxygen-carbon complexes.[12] These workers claim, based on HREELS experiments, that aluminum deposited onto oxygen-containing polymers reacts more with C—OH sites than with C=O sites.[12] Similar results have been obtained by other workers[11] for aluminum deposited within an XPS chamber onto polyimides. In this same reference it has also been shown that the aluminum, deposited onto polyimide at 300°C, actually penetrates the polymer to a depth of about 50 Å.

It has been demonstrated that stretching and heat setting temperatures can also significantly affect the level of adhesion obtained between aluminum and polyester.[12] The available published data, taken collectively, suggest that metallized systems have two components that contribute to the polymer/metal adhesion. One factor is chemical in nature while the other can be viewed as a mechanical contribution (mechanical interlocking). Toward understanding the greater level of adhesion observed for the copolymer-coated PET film compared with biaxially-oriented PET film analyses were performed. The experiments and results are discussed in the following sections.

EXPERIMENTAL

Polyester Films

Two types of polyester film were initially received from Hoechst Celanese Corporation (Polyester Film Products, Greer, SC, USA). These included a poly(ethylene terephthalate) film (Hostaphan 2400 series polyester film) and a poly(ethylene isophthalate-co-ethylene sodium sulfoisophthalate)-coated PET film. The copolymer thickness was estimated to be approximately 50 Å. These two films are hereafter referred to as PET and copolymer, respectively. Aluminized polyester films were also obtained from Hoechst Celanese Corporation. Films were prepared in a laboratory scale vacuum evaporator using different background pressures during the deposition (10^{-4} and 10^{-5} torr). A very thin coating of aluminum was obtained on these samples. These films were designated as VT (very thin) aluminum films. Some additional samples were prepared using industrial vacuum evaporation equipment with standard deposition parameters.

Aluminum Compounds

Three aluminum compounds were received from Aluminum Company of America (ALCOA) to aid the interpretation of X-ray photoelectron spectral data. The three compounds; Al_2O_3, AlOOH and $Al(OH)_3$, were analyzed by XPS as-received and also after vacuum drying at room temperature for 24 hours. Two additional compounds were also analyzed; aluminum acetate oxide ($Al_2O(CH_3COO)_4 \cdot 4(H_2O)$), obtained from Alfa Products, and aluminum carbide (Al_4C_3), obtained from the Aldrich Chemical Company. Both of these compounds were fine powders.

X-Ray Photoelectron Spectra

X-ray photoelectron spectra were obtained with a Perkin-Elmer Phi Model 5400 ESCA system using a magnesium anode ($K\alpha = 1253.6$ eV) at 400 W. Polyester film samples were attached onto stainless steel mounts with doublestick tape (3M Consumer Products Group, Cat. 137). The powdered aluminum compounds were pressed into Parafilm (American Can Company) which was then attached to the stainless steel sample mount with doublestick tape. The binding energies of the elements that were detected were referenced by positioning the lowest binding energy carbon C(1s) photopeak maximum at 284.8 eV.

Auger Electron Spectroscopy

Auger electron sputter depth profiles were obtained with a Perkin-Elmer Phi Model 610 Scanning Auger Microprobe System. A rastered area of 2 mm × 2 mm was evaluated. Samples were mounted similar to those prepared for XPS analysis except that the edges of the sample were coated with conductive paint to prevent excessive charge accumulation. The sputter rate was estimated to be 45 Å/minute based on the time required to penetrate the oxide coating of an aluminum specimen.

Transmission Electron Microscopy

Transmission electron micrographs were obtained with a Phillips Model 420 scanning transmission electron microscope. Samples prepared for TEM analysis were embedded in Electron Microscopy Sciences (EMS) ultralow viscosity resin (Cat. No. 14320) and were cured for approximately 8 h at 70°C. The samples were then sectioned to between 500 and 800 Å with a Reichert-Jung ultramicrotome using a Microstar diamond knife. The thin sections were placed on 300 mesh copper grids (EMS, Cat. No. T300 H-Cu) prior to examination.

Differential Scanning Calorimetry

Differential scanning calorimetry was used to evaluate the nonmetallized polyester films. A Perkin-Elmer Model DSC-4 differential scanning calorimeter was used with a heating rate of 20°C per minute for this work. All samples were encapsulated in standard aluminum pans. The ambient atmosphere was a dynamic nitrogen purge.

RESULTS AND DISCUSSION

Nonaluminized Polyester Controls

Prior to attempting to interpret the X-ray photoelectron spectra (XPS) obtained for aluminized samples, the spectra obtained for nonaluminized samples were carefully evaluated. The full width at half height, photopeak position at maximum intensity, and relative area of each peak were determined for both the PET and the copolymer-coated PET film. Further, the data obtained were compared with the values expected based on the reported chemical composition of the films and with the spectral data published by other workers.[13]

The average composition of the two types of films determined at a 90° takeoff angle (TOA) using XPS agrees very well with the expected composition (Table I). Qualitatively, PET film should, and does, have more oxygen and less carbon than the copolymer-coated PET film. Also, due to the sodium sulfonate substituent present in the copolymer, sodium and sulfur should be detected and have a calculated atomic ratio of 1:1. These two elements were detected at their approximate level of incorporation into the polymer and at close to the correct ratio. However, for both film samples there does appear to be slightly more carbon present than was expected.

The higher than expected level of carbon could be due to surface contamination or to different polymer repeat units. Usual sources of sample contamination include hydrocarbons, fluorocarbons and silicones that potentially originate from vacuum systems, ambient exposure and packaging materials. Silicon (present as silicone) would appear at a binding energy of approximately 102 eV.[14] No silicon, however, was detected on either film. Fluorocarbon contamination would have yielded a fluorine photopeak near 670 eV and a carbon C(1s) photopeak having a maximum intensity between 287.7 and 292.2 eV.[15] No fluorocarbon contamination was evident on the survey spectra.

A 15° TOA samples only about one-third of the depth that a 90° TOA samples (*i.e.* ~20 Å *vs* ~50 Å). Therefore, this shallower angle is more sensitive to surface contamination. Based on the data resulting from the 15° TOA (Table I) the greater

TABLE I
Atomic composition of nonaluminized polyester films

	Atomic concentration					
	PET film			Copolymer-coated film		
Element	Expected	90° TOA Found	15° TOA Found	Expected	90° TOA Found	15° TOA Found
Carbon	71.4	72.8	78.7	69.0	71.6	71.4
Oxygen	28.6	27.1	21.3	29.7	27.5	27.8
Sulfur	0.0	NA	NA	0.7	0.5	0.4
Sodium	0.0	NA	NA	0.7	0.4	0.4

NA, not analyzed

than expected carbon concentration that is observed is not due to the gross composition of the film but is instead due to surface contamination.

To assess more quantitatively the relative level of contamination and to obtain the photopeaks characteristic of nonaluminized samples the carbon and oxygen photopeaks were evaluated further. This was done so that any change in surface chemistry due to metallization that may occur could be documented. The carbon C(1s) photopeak can be very accurately described by four individual Gaussian photopeaks, each with a full width at half-maximum (FWHM) of 1.5 ± 0.1 eV. The positions of these four peaks were in agreement with the values expected based on the chemical structure of PET. The curve-resolved spectra and the relative areas of the peaks are shown in Figure 1.

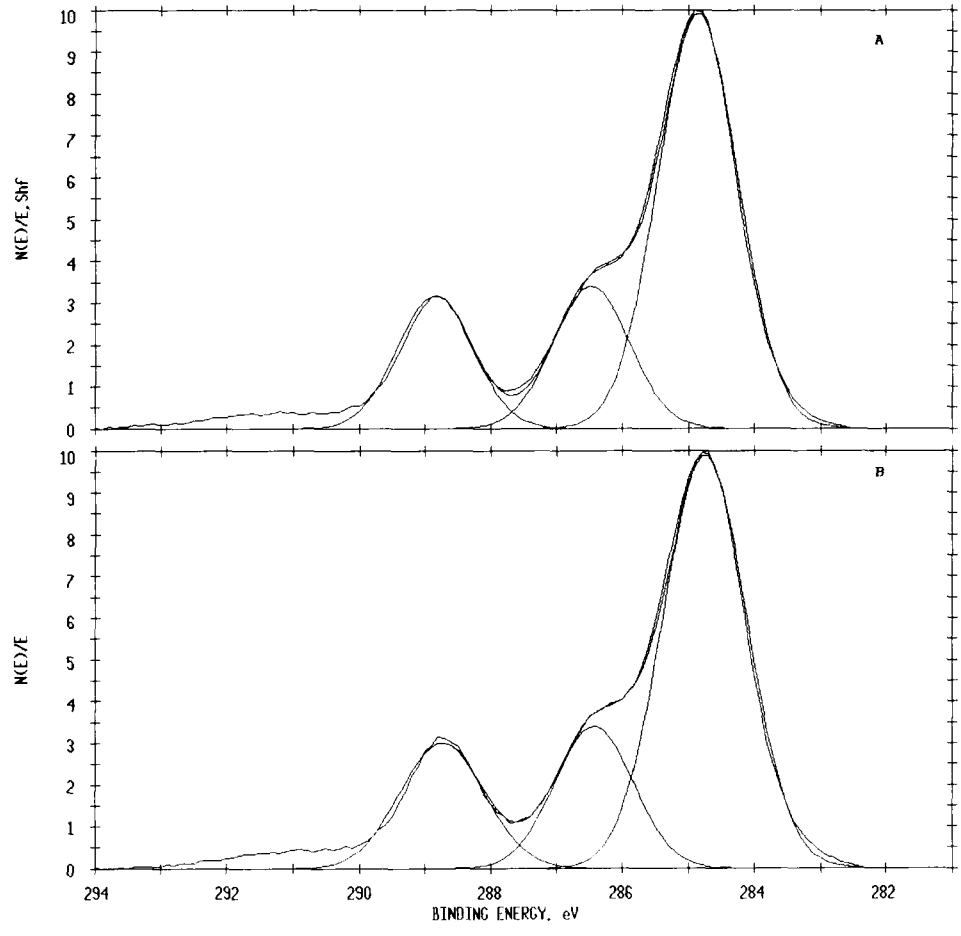

FIGURE 1 Curve-resolved carbon C(1s) photopeak for a PET film (A) and a copolymer-coated PET film (B).

Although Clark and Thomas[13] indicate four distinct carbon C(1s) photopeaks for PET, only three can actually be observed. This is due to the fact that two of the uniquely designated carbon atoms are actually identical when this monomer becomes a repeat unit in the polymer. Further, the natural dispersion of the non-monochromatized X-ray radiation precludes differentiating the other aromatic carbons from each other. A summary of the data pertaining to those carbon C(1s) photopeaks is found in Table II.

Both types of polyester film contain more of the lowest binding energy carbon than would be expected based on the areas of the photopeaks due to the C=O and C—O groups. As a reference for determining the areas expected for the photopeaks the C=O peak area was used. This peak was chosen because it was well resolved from the other C(1s) photopeaks. But, more importantly, it is expected that PET can contain excess C—O due to the incorporation of higher molecular weight glycols during polymerization. The excess carbon was estimated by multiplying the distinct C=O peak area by 3.0 (*i.e.* to obtain the aromatic contribution), adding this to the C=O and C—O peak areas, and subtracting the total calculated area of these three peaks from 100. For example, at a 15° TOA the PET film appears to have $100-[19.5+15.8+3(15.8)]=17.3\%$ carbon as contamination. At a 90° TOA the PET film had 8.5% excess carbon. The copolymer had 7.1 and 4.2% carbon contamination at a 15° TOA and a 90° TOA, respectively. This difference in surface contamination, if present at the time of metallization, could account for the superior adhesion observed with the copolymer-coated PET film.

The oxygen O(1s) photopeaks were also evaluated. For PET two individual photopeaks were expected[13] and were observed. The photopeak at highest binding energy is due to the O—C portion of the ester group, whereas the lowest binding energy photopeak is due to the O=C portion of the ester group. Their relative areas are in agreement with the carbon data presented previously. The positions of the peaks and their relative areas are shown in Table III. The presence of $-CH_2CH_2-O-CH_2CH_2-$groups should yield a peak with a binding energy that is approximately 0.3 eV lower than the —O—C=O peak. The curve fit is improved by the addition of a third peak which represents 4.7% of the total oxygen O(1s) peak area. This third peak does not improve the fit for the copolymer coating. It is

TABLE II
Carbon C(1s) photopeak information

		PET film			Copolymer-coated PET film		
Assignment	TOA	Binding energy (eV)	Relative area (%)	FWHM (eV)	Binding energy (eV)	Relative area (%)	FWHM (eV)
Aromatic C and hydrocarbon contamination	90	284.8	61.5	1.4	284.8	61.9	1.5
	15	284.8	64.7	1.5	284.8	60.5	1.5
C—O	90	286.5	20.6	1.4	286.5	20.0	1.4
	15	286.5	19.5	1.5	286.5	21.7	1.5
C=O	90	288.8	17.9	1.4	288.8	18.1	1.4
	15	288.9	15.8	1.4	288.8	17.8	1.5

TABLE III
Oxygen O(1s) photopeak information

		PET film			Copolymer-coated PET film		
Assignment	TOA	Binding energy (eV)	Relative area (%)	FWHM (eV)	Binding energy (eV)	Relative area (%)	FWHM (eV)
O=C	90(1)	532.0	47.1	1.6	531.9	51.7	1.7
	90(2)	531.9	49.7	1.6	531.9	52.7	1.7
O—C	90(1)	533.6	52.9	1.7	533.6	48.3	1.7
	90(2)	533.5	50.3	1.6	533.6	47.3	1.7

(1) and (2) denote two independent analyses

believed that the reason for this is that the oxygen atoms present in the $—SO_3$ group contribute to the lowest binding energy oxygen photopeak. The reported binding energy for oxygen in RSO_3Na is 532.0 to 532.2 eV.[16] The observed binding energy for the oxygen O(1s) photopeak of the O=C portion of an ester is 531.9 eV. Thus, the $—SO_3$ cannot be resolved confidently from the O=C—photopeak even though the sulfonate group probably skews the photopeak (making it nonGaussian). Because of the low concentration of the sulfonate group and the similarity of its binding energy to the —C=O group, additional interpretation of the oxygen photopeak by XPS for nonaluminized polyester samples was not pursued.

A final evaluation of the previously-discussed data was performed to assess the internal consistency of the data in terms of the relative concentrations of functional groups. The average gross composition (albeit the surface region) and the curve-resolved photopeak data obtained at a 90° TOA were utilized (Table IV). For the PET film the agreement between the relative concentrations of specific functional groups, based on the independent, curve-resolved carbon and oxygen spectra, is very good (~4% relative difference). The copolymer-coating does not yield data that are as strongly self-consistent (~9% relative difference). This is probably due to the $—SO_3$ that had not been directly accounted for. These relative difference values were used to set limits for changes in chemical functional group concentrations that may be considered significant for aluminized polyester films.

TABLE IV
Absolute concentration of functional groups in polyester films (90° TOA), mole percent

Functional group	PET film	Copolymer-coated PET film
C=O (C)	13.0	13.3
C=O (O)	13.1	14.6
C—O (C)	14.5	14.6
C—O (O)	14.0	13.4

Note: (C) indicates entry is based on curve-resolved carbon photopeak
(O) indicates entry is based on curve-resolved oxygen photopeak

Deviation from the idealized PET chemical repeat unit was also evaluated as a potential contribution to the increased carbon level. Specifically, the presence of either diethyl ether or butylene groups could change the carbon concentration. The presence of only diethyl ether groups would actually decrease the expected carbon concentration from 71.4 to 70.6 atomic percent. This difference is not large enough to consider significant without additional analyses. The PET film would have to be 78% poly(butylene terephthalate) to explain the average carbon concentration of 72.9% that was observed. This is not consistent with the physical properties of the films. Thus, based on the chemical constituents indicated by the survey spectra and on the atomic composition data, it is most probable that the surfaces of the two types of polyester contain different amounts of hydrocarbon contamination.

Aluminized Polyester Films

Samples were intentionally prepared using short enough deposition times that a very thin (VT) coating of aluminum was obtained. Using these samples (VT films) information pertaining to the aluminum/polyester interface has been obtained. X-ray photoelectron spectroscopy indicates that these samples do not contain any aluminum metal because the metal would have yielded a distinct aluminum Al(2p) photopeak with a binding energy of 72.9 eV (Figure 2). To aid in the identification of the species that were present on the surface of these films reference samples of Al_2O_3, AlOOH, $Al(OH)_3$ and $Al_2O(CH_3COO)_4 \cdot 4H_2O$ were analyzed by XPS. The aluminum and oxygen photopeaks were evaluated for these compounds (Table V). The carbon photopeak was also evaluated for the aluminum acetate oxide. The data indicate that the oxygen O(1s) photopeak distinguishes AlOOH and aluminum acetate oxide from either Al_2O_3 or $Al(OH)_3$ but the latter two compounds cannot be distinguished from each other based on the position of the O(1s) photopeak. The Al(2p) photopeak, in combination with the O(1s) photopeak position, does distinguish Al_2O_3 from $Al(OH)_3$. The aluminum acetate oxide has two distinct carbon C(1s) photopeaks at 289.3 and 284.8 eV. These peaks are interpreted as being due to Al—O—$\underline{C}H_2$— and —$\underline{C}H_3$, respectively. Further, they are present at close to the expected peak area ratio of 1:1.

The surface composition of the aluminized (VT) films is shown in Table VI. For reference, industrially-prepared samples had 30 to 38 atomic percent aluminum on their surface. It is apparent that, as desired, a very small amount of aluminum has actually been deposited on the laboratory-prepared specimens. No direct correlation of the amount of aluminum with the XPS TOA can be made because the XPS samples were obtained from random positions on the circular samples. These samples, at the heavier levels of aluminization, were visually nonuniform. Therefore, it is expected that aluminum content varies with sampling position. Based on the aluminum photopeak binding energy (~74.8 eV) the aluminum appears to be present predominantly as Al_2O_3.

The most noteworthy observation pertaining to these films was that the oxygen O(1s) photopeak for the aluminized (VT) films contained functionalities that were not present in the base film (Figure 3A). Of course, one would expect a new functionality due to the oxygen atoms present in the aluminum oxide. Because both the nonaluminized polyester films and several aluminum oxide standards were evalu-

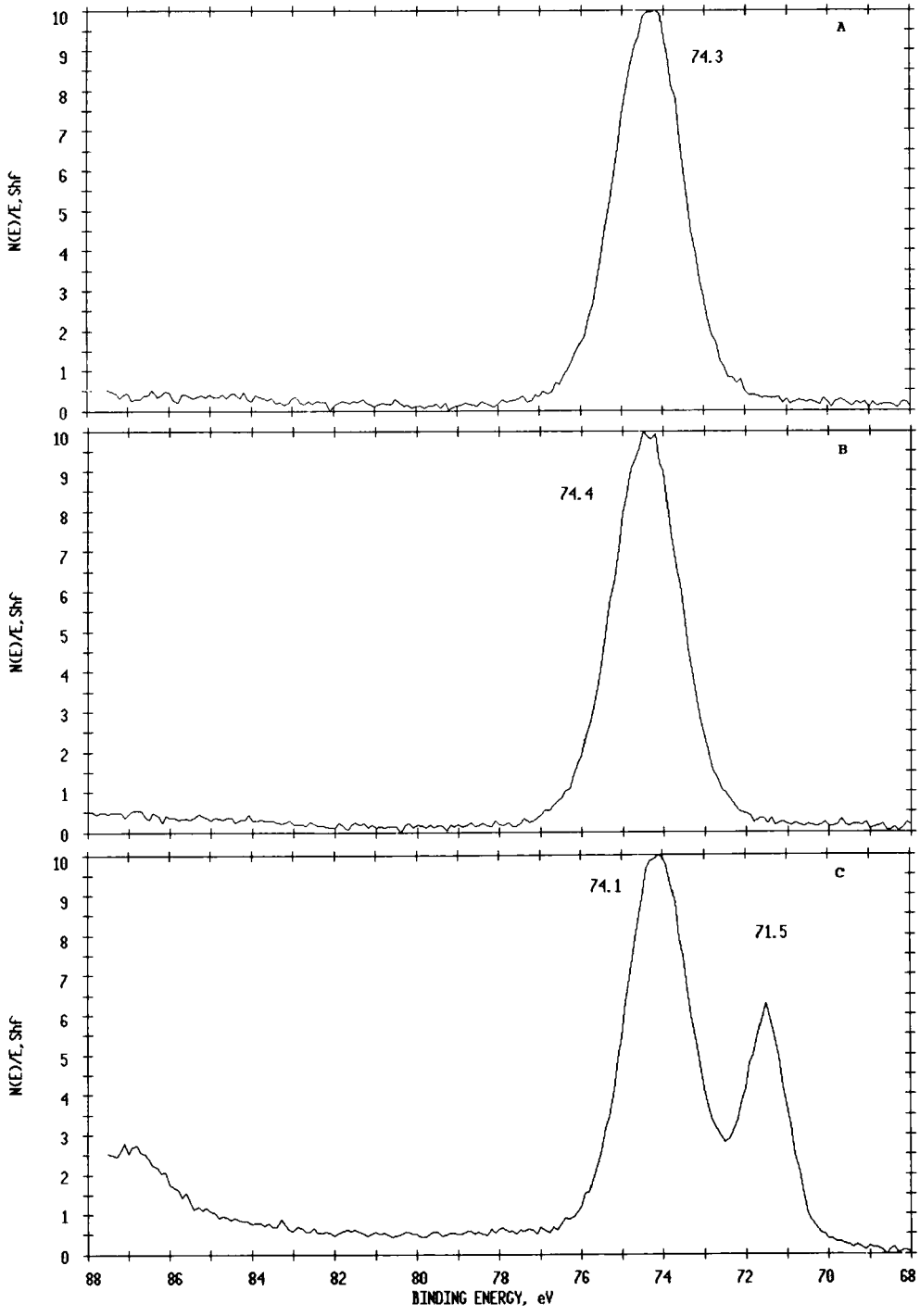

FIGURE 2 Aluminum Al(2p) photopeak observed for a PET film (A), a copolymer-coated PET film (B) that were vacuum evaporated with a thin coating of aluminum and a PET film having a thick aluminum coating (C).

TABLE V
Data pertaining to aluminum compounds
(Vacuum dried 24 h at room temperature and pressed into parafilm)

Sample	Atomic concentration (%)			Binding energy (eV)		
	Carbon	Oxygen	Aluminum	Carbon	Oxygen	Aluminum
Parafilm	99.7	0.3	—	284.8	532.0	—
AlOOH	8.9	64.3	26.8	284.8	531.5	73.9
$Al(OH)_3$	17.6	61.5	20.9	284.8	531.8	74.1
Al_2O_3	38.7	36.9	24.4	284.8	531.7	74.6
$Al_2O(CH_3COO)_4 \cdot 4H_2O$	33.5	53.8	12.6	284.8 289.3	532.4	74.4

TABLE VI
Surface composition of polymer films with a very thin aluminum deposit (VT films)

Sample	TOA	Surface composition (atomic percent)				
		C	O	S	Na	Al
PET	90	41.7	44.3	NA	NA	13.9
	45	55.8	35.9	NA	NA	8.3
	15	55.8	30.1	NA	NA	14.2
Copolymer-coated PET	90	30.2	49.2	0.2	1.2	19.2
	45	39.3	44.1	0.2	0.5	15.9
	15	50.0	34.0	NA	NA	16.1

ated, confident oxygen photopeak assignments could be made. The fit of the oxygen O(1s) photopeak with two peaks of equal area due to the C—O and C=O moieties and a third peak due to Al_2O_3 yields an obvious deficiency (Figure 3B). Adding a fourth peak, approximately midway between the C—O and C=O peaks, results in much closer agreement between the expected total O(1s) photopeak and the experimental data (Figure 3C). This peak is at a position nearly identical to the position of the O(1s) photopeak observed with the aluminum acetate oxide standard. At each of three take-off angles both types of aluminized (VT) polyester films were similarly analyzed. The results of the curve-resolved oxygen O(1s) photopeaks are shown in Table VII. For each, a substantial amount of this fourth type of oxygen is required to curve-fit the total O(1s) photopeak accurately. Nonaluminized PET could be curve-fit with the same peak but its relative area was only 3–5%. Because of concern that this peak may really be due solely to the aluminum oxide and not be indicative of polymer degradation or reaction of the PET with the deposited aluminum, additional work was performed with the aluminum standards.

Evaluating a sample of Al_2O_3 powder, as-received, by XPS was informative. The oxygen photopeak observed for dried Al_2O_3[16] was positioned within the O(1s) photopeak actually observed with the sample as-received and the peak intensity was maximized (Figure 4). It is obvious that there is a large oxygen-containing species not accounted for, but its position is at a lower binding energy than the Al_2O_3 peak.

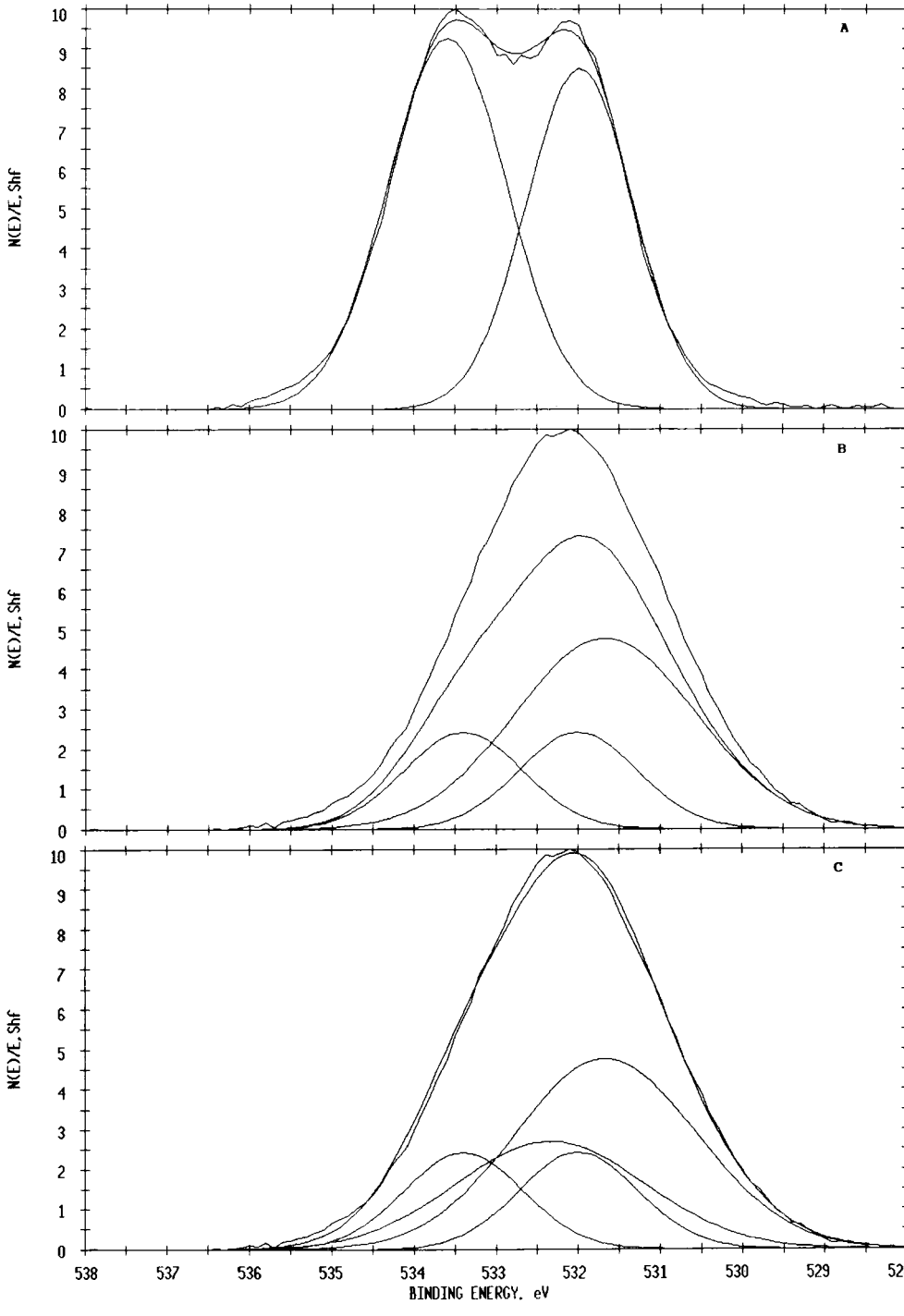

FIGURE 3 Curve-resolved oxygen O(1s) photopeak for a PET film before (A) and after vacuum evaporation with aluminum; three-peak fit (B) and four-peak fit (C).

TABLE VII
Summary of oxygen photopeak data obtained from polymer films with a very thin (VT) aluminum deposit

Sample	TOA	Relative peak areas			
		O—C	New	O=C	Oxide
PET	90	14.8	26.1	14.7	44.4
	45	26.2	24.7	23.1	26.0
	15	12.0	17.0	12.8	58.3
Copolymer-coated PET	90	8.9	37.1	10.5	43.5
	45	9.1	28.5	10.6	51.8
	15	5.1	29.1	6.6	59.3

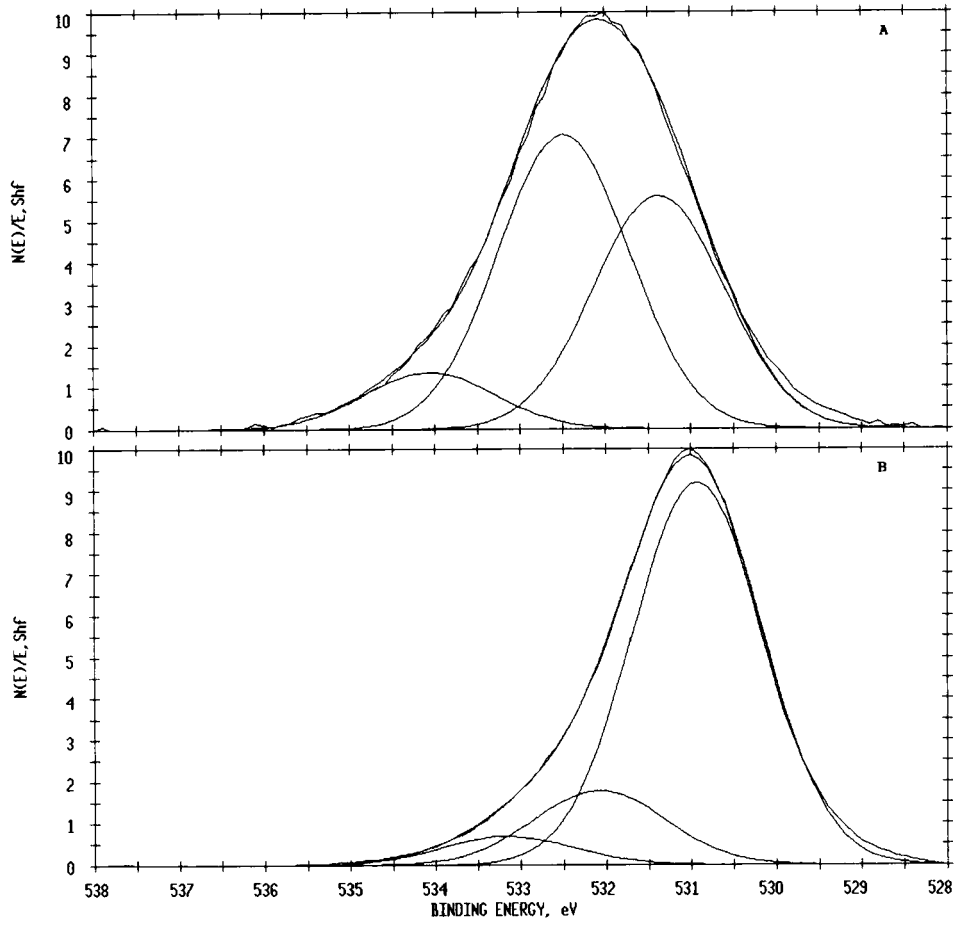

FIGURE 4 A comparison of the oxygen O(1s) photopeak for Al_2O_3 after vacuum drying (A) and as-received (B).

This is the opposite direction with respect to the new oxygen functionality that was utilized to curve-fit the oxygen photopeak of aluminized (VT) films. Similar results were obtained for the AlOOH sample. It is believed that this lower binding energy O(1s) photopeak is due to adsorbed water.

Based on the position of the photopeak due to the new oxygen functionality and the fact that it is not due directly to the aluminum oxide, the XPS data were further evaluated. It would be expected, based on one of the operating principles of XPS, that if an oxygen photopeak with a position midway between the O—C and O=C photopeaks is observed then a carbon photopeak midway between the C—O and C=O photopeaks should also be observed if the new oxygen is simply part of an organic moiety.

The carbon C(1s) photopeaks for the aluminized (VT) polyester films were curve fit with five photopeaks (Figure 5C). In no case did the relative peak area of the "new carbon" photopeak exceed 2.0%. In the nonaluminized polyester films a peak midway between C—O and C=O had a relative area of only 1%. This is too low to be related to the new oxygen functionality that was previously discussed. Thus, it is postulated that this new functionality is not a simple organic functionality but is instead due to an organoaluminum species.

Based on the discussion above, it appears that the most reasonable interpretation of the oxygen XPS data for the aluminized polyester films is the following:

(1) Upon vacuum evaporation of aluminum metal onto or into the polyester films some surface degradation occurs. This results in a vinyl endgroup and a carboxylic acid endgroup. The carbon and oxygen XPS photopeak positions for the carboxylic acid moiety would not be distinguishable from the ester moiety. The formation of a vinyl endgroup would increase the relative intensity of the lowest binding energy carbon photopeak.
(2) Subsequent reaction of the aluminum with the carboxylic acid endgroup and oxidation by adsorbed atmospheric water or moisture that has diffused through the polyester film could yield an aluminum carboxylate oxide species.

Data pertaining to the carbon C(1s) spectrum that had been curve resolved with four photopeaks were also obtained (Figure 5). It appears that the concentrations of each type of carbon-containing group are similar for both types of aluminized (VT) polyester film. However, the relative area of the carbon 1s photopeak at 284.8 eV has increased for aluminized films (Table VIII). Specifically, the ratio of C=C to either C—O or C=O is greater than the expected value of 3. This increase can be explained by the formation of a new functionality at low binding energy, a carbidic functionality.

Support for the existence of a carbidic functionality comes from the carbon C(1s) photopeak of aluminum carbide on Parafilm (Figure 5). A small amount of sample was intentionally placed onto Parafilm to obtain an internal hydrocarbon standard (Table V). The curve-resolved photopeak shows the contribution from Parafilm as a photopeak at 284.8 eV, and another photopeak at 283.8 eV, due to the aluminum carbide. Thus, the carbon in aluminum carbide exhibits a distinct photopeak ~1.0 eV lower than hydrocarbon or aromatic carbon.

In order to evaluate the applicability of the aluminum carbide XPS data to the

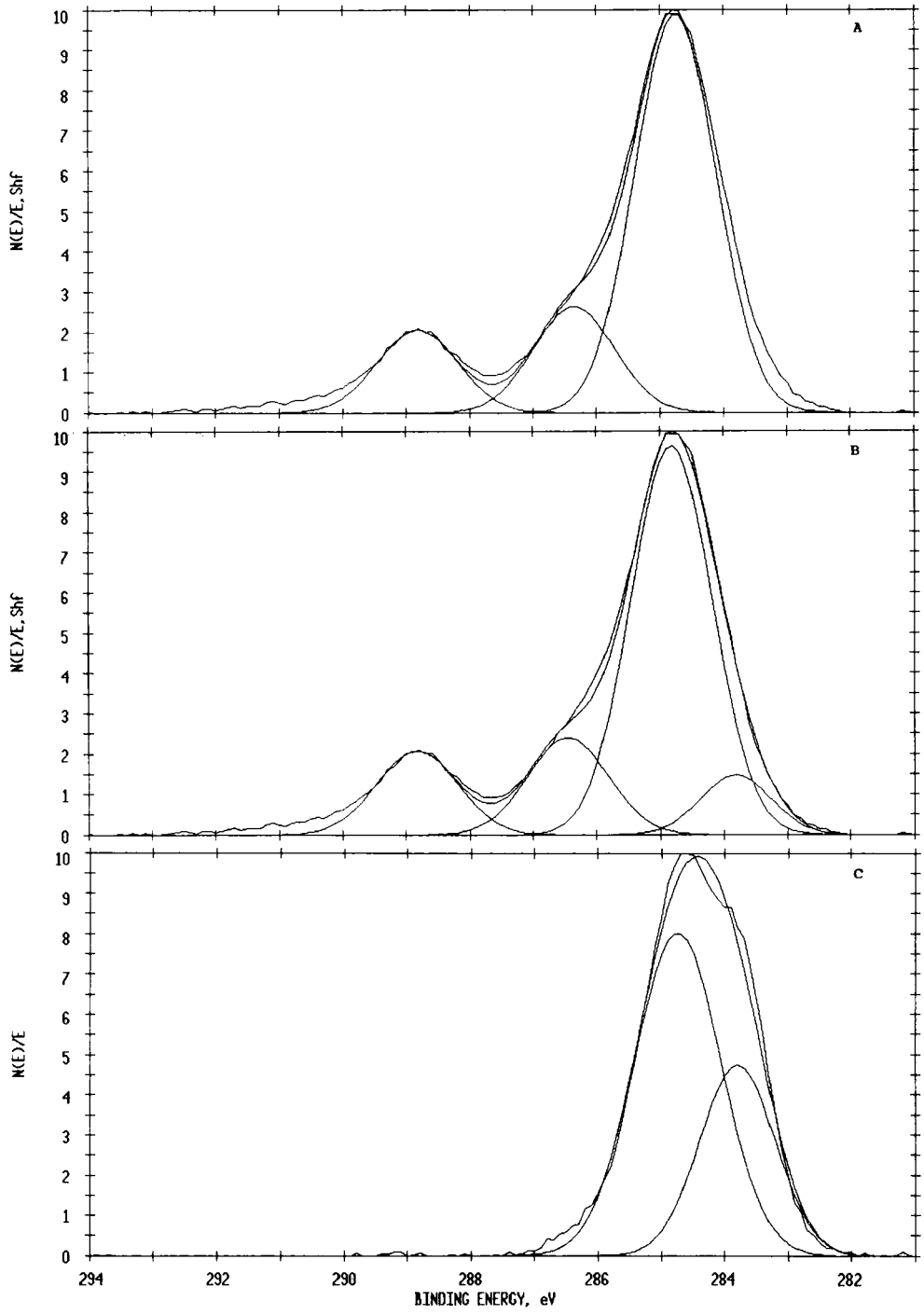

FIGURE 5 Curve-resolved carbon C(1s) photopeak for PET film vacuum evaporated with aluminum; three-peak fit (A) and four-peak fit (B). Carbon C(1s) photopeak for aluminum carbide (C).

TABLE VIII
Curve-resolved carbon 1s photopeak for polyester films with and without a very thin (VT) aluminum deposit

Sample	TOA	Relative peak areas			
		C=C	C—O	C=O	C—Al
PET	90	62.6	15.6	13.5	8.3
	45	61.0	20.5	15.4	3.2
	15	70.2	11.9	5.9	12.0
Copolymer-coated PET	90	64.4	16.4	13.2	5.9
	45	66.3	12.9	9.2	11.7
	15	73.4	11.3	5.6	9.8
PET Alone	90	55.7	23.6	18.5	2.2*
Copolymer-coated PET Alone	90	56.5	22.3	18.8	2.5*

*These values are reported to provide a reference value for the amount of carbide functionality that may be indicated by the curve-fit routine for a sample that has no carbide functionality.

aluminized (VT) polyesters, the carbon C(1s) data from both types of films were evaluated to include a peak at ~283.8 eV. The results (Table VIII) indicate a significant amount of carbidic carbon in all samples. The data do support the presence of aluminum carbide-like and aluminum carboxylate species at the interface of aluminum on polyester films.

Additional films that contained slightly thicker deposits of aluminum were similarly evaluated. The surface composition of these films was determined by XPS. The curve resolution of the carbon and oxygen photopeaks for these films yielded comparable results to those presented above. Therefore, these samples are not specifically discussed further.

Fourier-transform infrared spectrometry was applied to nonaluminized films and to the polyester films that had a very thin aluminum deposit. The ATR mode was used at both 60° and 45° angles. No significant differences could be detected between copolymer-coated PET film and the conventional PET film, between the VT films, or between any other appropriate pairs of samples. This is due to the fact that the depth that this technique samples is still fairly large with respect to the thickness of the copolymer layer or aluminized layer. It has been reported that the minimum thickness of an organic layer on an IR absorbing substrate that can be reliably evaluated with FT-IR/ATR is ~10 Å.[17]

Industrially-Prepared Samples

Industrially-prepared samples indicated an aluminum metal peak in addition to aluminum oxide (Figure 2C). This observation implies that the aluminum deposit is greater than 50–75 Å thick. Transmission electron micrographs obtained with ultramicrotomed cross-sections of these films indicated that the metal deposit is actually 400–800 Å thick. Thus, XPS could not be used to probe directly the aluminum-polyester interface in the case of these industrially-prepared samples.

To determine if the aluminum layer was more diffuse (broader interphase) in the case of the copolymer, compared with the PET film, Auger electron spectroscopy

with depth profiling *via* argon ion etching was used. The thickness of the metal layer directly determined by TEM, divided by the sputter time required to reach 50% of the maximum carbon signal, was used to estimate the sputter rate (approximately 45 Å/min). The interphase width was estimated[18] from the 16% to 84% values of the maximum carbon signal attained (Figure 6). The data indicate that for a given deposition pressure the substrate does not yield a significantly different interphase width (200–300 Å on average).

Further TEM evaluation of these samples did indicate a difference in the depth to which the metal is deposited into the polyester. It appears that the aluminum penetrates the copolymer coating to a depth equal to the estimated copolymer thickness of 50–75 Å (Figure 7). It is reasonable that the aluminum should penetrate the copolymer more than the PET based on the relative thermophysical properties of these two polymers. The copolymer is more amorphous and has a lower glass transition temperature and melting temperature than that of PET (75° *versus* 81°C and 201° *versus* 244°C, respectively). It therefore appears that the aluminum may adhere better to the copolymer than to the PET due to enhanced mechanical interlocking in the former.

CONCLUSIONS

Adhesion of vacuum-evaporated aluminum to PET and to copolymer-coated PET film is due to chemical and/or mechanical reasons. Evidence that, for these systems, both mechanisms are operating was obtained by using spectroscopic, microscopic and thermoanalytical techniques. Carbon and oxygen XPS spectra of the nonaluminized polyester substrates could be very accurately curve fit. The peak positions were chemically interpretable and were in close agreement with literature values. Upon metallization two new oxygen functionalities were created; one was due to aluminum oxide and the other to an aluminum carboxylate oxide species. This assignment is consistent with the known thermal decomposition pathway of polyesters and is chemically reasonable. Curve-resolution of carbon C(1s) spectra also suggests the formation of a carbidic species with aluminum, evidenced by a lower binding energy photopeak. For all aluminized samples similar levels of the new functionalities were observed. It, therefore, appears that covalent bonding between the aluminum and the polyester is occurring, but to similar levels in both types of films. Thus, neither the new oxygen functionality nor the carbidic carbon alone can be responsible for the enhanced adhesion observed with copolymer-coated PET film.

Significantly different levels of surface contamination were indicated based on the curve-resolved XPS C(1s) carbon photopeaks for nonaluminized polyester films. The conventional PET film had more than twice as much contamination as the copolymer-coated PET. This alone, if present at the time of metallization, could explain the differences in adhesion that are observed.

The transmission electron micrographs obtained from commercially-aluminized polyester films indicated that the aluminum penetrated the copolymer-coating to a depth approximately equal to its thickness. Very little penetration of the PET by

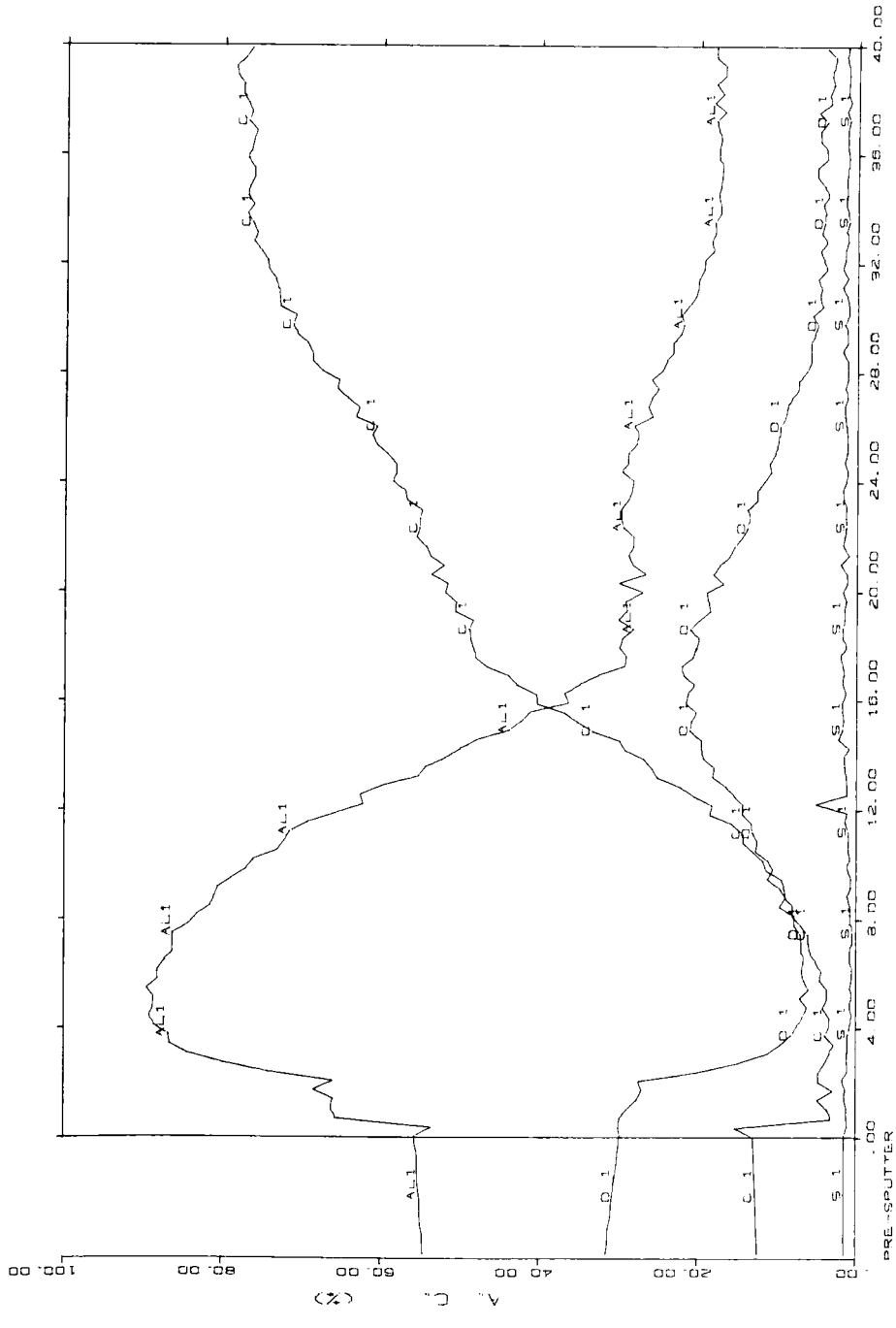

FIGURE 6 An Auger electron spectroscopy depth profile for an industrially-aluminized Al-PET sample.

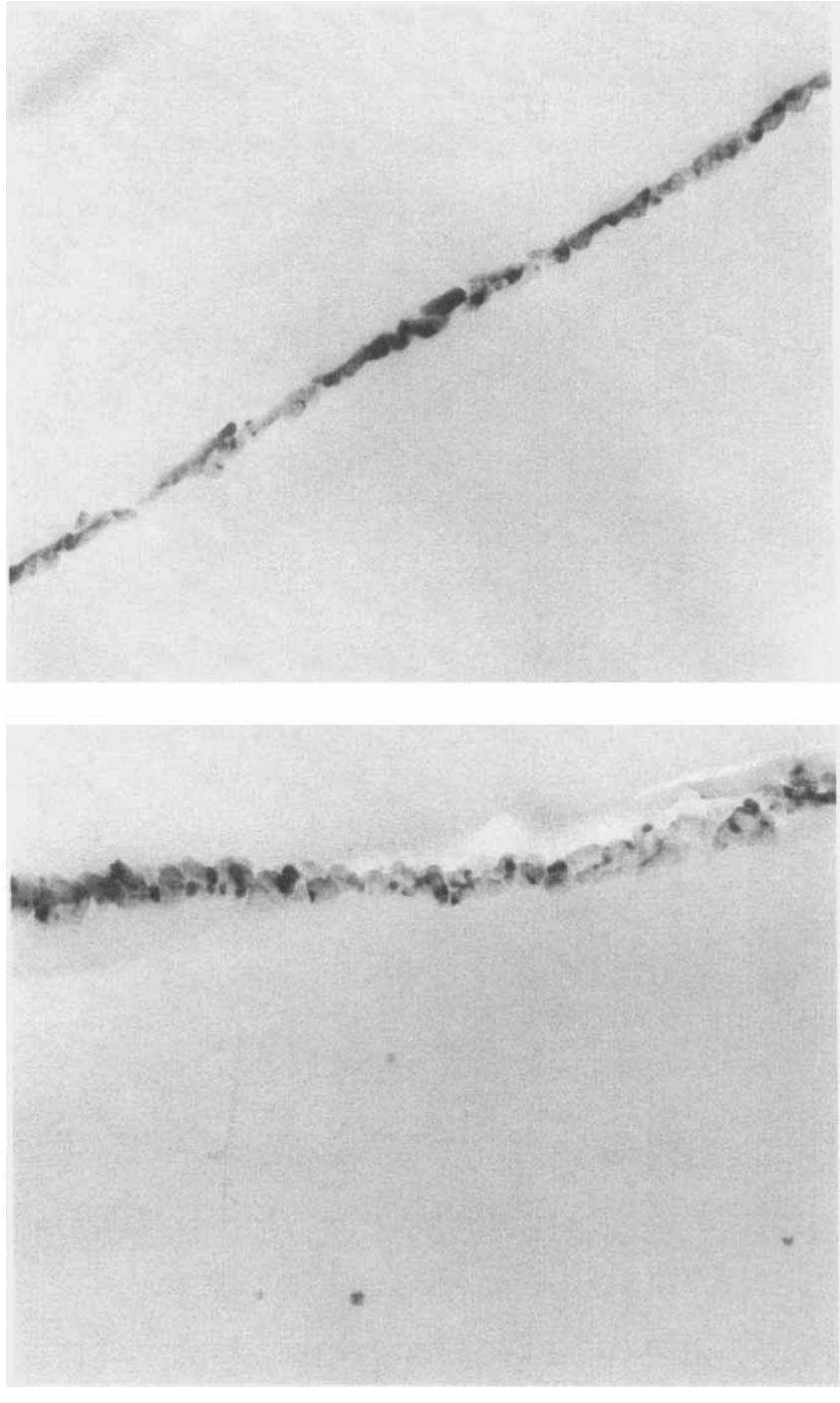

a

b

FIGURE 7 Transmission electron micrographs of industrially-aluminized PET (A) and copolymer (B).

the aluminum was evident. The greater penetration into the copolymer compared with the PET is reasonable due to the lower crystallinity, lower glass transition temperature and lower melting point of the copolymer. This enhanced mechanical interlocking that results with the copolymer, together with chemical reaction with both types of films appears to explain the differences in adhesion that were observed.

Acknowledgements

The authors gratefully acknowledge the financial support of this work by Hoechst Celanese Corporation, Polyester Films Division, Greer, South Carolina, U.S.A. The technical contributions and preparation of samples by Dr. Ed Culbertson and his colleagues at Hoechst Celanese were very helpful. Finally, we thank Ms. Sharon L. Edie for the large amount and diversity of initial work that she contributed to this project.

References

1. S. Wu, *Polymer Interface and Adhesion* (Marcel Dekker, NY, 1982).
2. Minnesota Mining & Manufacturing Co., Brit. Patent, 891, 469 (March 14, 1962).
3. L. E. Wolinski, E. I. DuPont de Nemours & Co., U. S. Patent 3,274,089 (September 16, 1966).
4. I. A. Abu-Isa, *Polym. Plast. Technol. Eng.*, **2,** 29 (1973).
5. R. A. Bragole, *Adhesives Age,* **17,** 24 (1974).
6. J. M. Burkstrand, *J. Vac. Sci. Technol.*, **21,** 70 (1979).
7. W. R. Combotz and A. S. Hoffman, *Polym. Mater. Sci. Eng.*, **56,** 720 (1987).
8. D. Satas, in *Plastics Finishing and Decoration,* D. Satas, Ed. (VanNostrand Reinhold Co., NY, 1986), p. 70.
9. F. G. Funderburk, E. C. Culbertson and R. G. Posey, American Hoechst Corp., U. S. Patent 4,493,872.
10. C. A. L. Westerdahl, J. R. Hall, E. C. Schramm and D. W. Levi, *J. Colloid. Interface Sci.*, **47,** 610 (1974).
11. D. J. Brown, *Thin Solid Films,* **147,** 105 (1987).
12. T. H. Duc and Y. Jugnet, Int. Conf. on Adh. and Surf. Anal., April 1990, Loughborough University of Technology, UK.
13. D. T. Clark and H. R. Thomas, *J. Polym. Sci. Polym. Chem. Ed.*, **16,** 791 (1978).
14. Handbook of X-ray Photoelectron Spectroscopy, Wagner *et al.*, Perkin-Elmer Corp., Eden Prairie MN, U.S.A. (1979), p. 52.
15. *Ibid.*, p. 44.
16. *Ibid.*, p. 42.
17. K. Ohta and R. Iwamoto, *Anal Chem.*, **57,** 2491 (1985).
18. Y. DePuydt, P. Bertrand and P. Lutgen, *Surf. Interface Anal.*, **12,** 486 (1988).